

# VRED: A Position-Velocity Recurrent Encoder-Decoder for Human Motion Prediction

Hongsong Wang Jiashi Feng

Department of Electrical and Computer Engineering,  
National University of Singapore

hongsongsui@gmail.com, elefjia@nus.edu.sg

## Abstract

Human motion prediction, which aims to predict future human poses given past poses, has recently seen increased interest. Many recent approaches are based on Recurrent Neural Networks (RNN) which model human poses with exponential maps. These approaches neglect the pose velocity as well as temporal relation of different poses, and tend to converge to the mean pose or fail to generate natural-looking poses. We therefore propose a novel Position-Velocity Recurrent Encoder-Decoder (PVRED) for human motion prediction, which makes full use of pose velocities and temporal positional information. A temporal position embedding method is presented and a Position-Velocity RNN (PVRNN) is proposed. We also emphasize the benefits of quaternion parameterization of poses and design a novel trainable Quaternion Transformation (QT) layer, which is combined with a robust loss function during training. Experiments on two human motion prediction benchmarks show that our approach considerably outperforms the state-of-the-art methods for both short-term prediction and long-term prediction. In particular, our proposed approach can predict future human-like and meaningful poses in 4000 milliseconds.

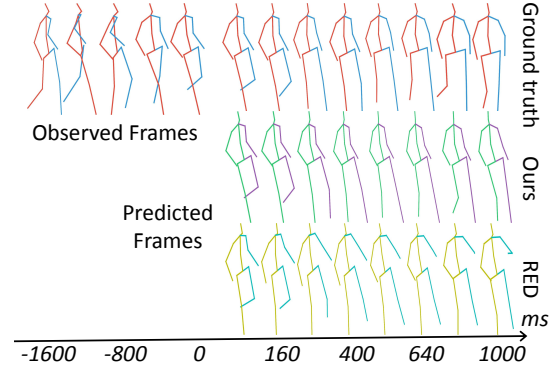


Figure 1. Human motion prediction with different models. Given observations of past frames, the goal is to predict future frames of human poses in the next 1,000 milliseconds. We observe that the predictions from our proposed model are more accurate and natural than those of RED [19]. Note that images of different poses are resized to the same size for better visualization.

is not so deterministic in the distant future, thus making it even more difficult for long-term ( i.e. more than 400 milliseconds) prediction.

Traditional approaches for learning dynamics of human motion mainly use probabilistic models including hidden Markov model [3], linear dynamic system [21] and restricted Boltzmann machine [25]. Prior knowledge about human motion is typically imposed and statistical models are used to constrain pose dynamics. Imposing physics based constraints is difficult and complex. Also, these approaches either generate unrealistic human motion or result in intractable estimation and inference problems.

Deep learning has also been successfully applied in human motion prediction. A family of methods based on Recurrent Neural Networks (RNN) are proposed, e.g., encoder-recurrent-decoder [7], structural-RNN [15] and RNN with de-noising autoencoder [9]. These models learn structural and temporal dependencies from the training data and directly predict future poses. However, they tend to converge to the mean pose or fail to generate natural-looking poses. Martinez et al. [19] proposed Recurrent

## 1. Introduction

Human motion prediction aims to predict the future human motion dynamics given the past motion data. It has various applications including human-robot interaction [2], augmented reality [27], animation [13], etc. The temporal changes of human poses show motion dynamics of the whole body. One common task of this problem is to forecast the most likely future 3D poses of a person by learning models from sequences of 3D poses. The task is challenging due to the non-rigid movement of articulated human body and the multimodal motion data, e.g., the sequence of an activity that may consist of several submotions. The human pose

Encoder-Decoder (RED) with residual connections that predicts velocities of body joint motion rather than poses. This approach mitigates the mean pose problem but may produce inaccurate and unnatural poses for long-term predictions (see results of RED in Figure 1).

Another disadvantage of RED based approaches is that the decoder RNN neglects temporal relations between poses of different frames due to autoregression based prediction. To address this issue, inspired by position embedding widely used in natural language processing [26, 8], we aim to design a network which could encode temporal relative positions of different frames.

For representing 3D human poses, the widely used parameterization schemes include the Euler angle, exponential map and quaternion [10]. The exponential map is the most popularly adopted but it suffers from singularities (i.e., gimbal lock) and discontinuities of joint angles [10]. The quaternion parameterization is free of singularities and discontinuities of the representation, and would gain a more practical insight into human motion prediction. These advantages have been confirmed by the recently proposed QuaterNet [20] which employs quaternion to represent the input pose. However, QuaterNet abandons the raw input of exponential maps and also requires additional operations of preprocessing and postprocessing. An end-to-end network that makes full use of the quaternion parameterization is still absent.

Taking the pose velocities, relative position encoding and quaternion parameterization into consideration, we propose a novel end-to-end trainable network, termed as Position-Velocity RED (PVRED), for human motion prediction. Different from previous methods [9, 24, 5, 18], our proposed network takes in three types of input: human poses, pose velocities and position embedding. To differentiate representations of adjacent and similar frames, we present an effective position embedding method based on sine and cosine functions of different frequencies to encode temporal positions of different frames. We design a Position-Velocity RNN (PVRNN) which constitutes the main part of PVRED. PVRNN takes in the three inputs and predicts pose velocities, which are then added to the previous poses to get the future poses. For the decoder, predictions of pose velocities and human poses are used as input for the next time step. To make use of the benefits of quaternion parameterization of 3D poses, we design a novel Quaternion Transformation (QT) layer to convert predicted poses from exponential maps to quaternion. The QT layer is embedded into the end-to-end trainable network. We also define a mean absolute error loss in the unit quaternion space to minimize the differences between the observed and predicted poses.

We make the following contributions. First, we propose a novel Position-Velocity Recurrent Encoder-Decoder (PVRED) for human motion prediction. Second, we first

exploit temporal position embedding over frames while modeling the human pose sequences. Third, we design a novel Quaternion Transformation (QT) layer which could take advantages of quaternion parameterization of 3D pose for better pose prediction. Finally, our method obtains the state-of-the-art results for both short-term and long-term prediction of human motion with periodic actions as well as aperiodic actions.

## 2. Related Work

Predicting human motion dynamics is related to a range of research topics. Here we only review the previous works that are most related to ours.

**Human Motion Prediction.** Owing to the development of sequence-to-sequence models [6, 23], several Recurrent Neural Networks (RNN) based approaches are proposed for human motion prediction. Fragkiadaki et al. [7] proposed a recurrent architecture that incorporates nonlinear encoder and decoder networks. Jain et al. [15] developed a method for casting an arbitrary spatio-temporal graph as a fully differentiable and trainable RNN structure. Martinez et al. [19] presented a simple and effective baseline by adding a residual connection between the input and the output of each RNN cell. Ghosh et al. [9] combined a de-noising autoencoder with a 3-layer RNN to model the temporal aspects and recover the spatial structure of human pose. Recently, Gui et al. [11] proposed a geodesic loss to incorporate local geometric structure constraint and introduced two global recurrent discriminators to validate the plausibility of predictions. Pavllo et al. [20] designed an RNN architecture based on quaternions for rotation parameterization which shows the advantage of quaternions over exponential maps.

There are also some approaches beyond the RNN based ones. Bütetage et al. [4] proposed fully-connected networks with a bottleneck and directly fed the recent history poses to the model. Li et al. [18] utilized Convolutional Neural Networks (CNN) to learn to capture both invariant and dynamic information of human motion.

These approaches mostly model the exponential map of human poses, and neglect temporal relations of poses at different time steps. Our approach belongs to the paradigm with RNN and outperforms all the previous approaches by taking full advantage of human poses, pose velocities and position embedding of different frames.

**Probabilistic Models.** Besides the deep learning based human motion prediction, there are some probabilistic models of human motion which can be applied in motion completion [17], 3D action recognition [28, 29], etc. Brand et al. [3] used a hidden Markov model to generate new motion sequences of different styles. Pavlovic et al. [21] proposed switching linear dynamic system models to learn dynamic behaviour. Sidenbladh et al. [22] presented an implicit probabilistic model to provide a prior probability distribu-

tion over human motions. Lehrmann et al. [16] introduced a non-parametric Bayesian network to generalize the prior of human pose with estimation of both graph structure and its local distribution. Wang et al. [30] introduced a gaussian process dynamical model which comprises a latent space and a map from the latent space to an observation space. Taylor et al. [25] used a conditional restricted Boltzmann machine to learn local constraints and global dynamics of human motion. Lehrmann et al. [17] introduced the dynamic forest model which models human motion with an expressive Markov model.

These works exploit the low-dimensional representation of human motion with probabilistic models, while our approach obtains this representation using deep networks which could synthesize realistic motion sequences.

### 3. Preliminaries

In this section we revisit the RNN Encoder-Decoder (RED) paradigm and its application in human pose estimation as preliminaries.

#### 3.1. RNN Encoder-Decoder

An RNN is a neural network that consists of a hidden state which operates on an input sequence of variable length. Given the input sequence  $X$  with length  $m$ , i.e.,  $X = (x_1, \dots, x_m)$ , where  $x_t$  is the input at time step  $t$ , the hidden state  $h_t$  is updated by

$$h_t = f(h_{t-1}, x_t) \quad (1)$$

where  $f$  is a non-linear activation function. The standard RNN suffers from the vanishing gradient problem, and some improved structures including Gated Recurrent Unit (GRU) [6] and Long Short-Term Memory (LSTM) [12] are designed by utilizing a gating mechanism.

The RNN Encoder-Decoder (RED) [6, 23] is a neural network architecture that consists of two RNNs, i.e., the encoder RNN and the decoder RNN. It first encodes an input sequence into a fixed-length vector representation and then decodes this vector into a new output sequence. Both the input sequence and the output sequence have a variable length. Suppose the input sequence is  $X = (x_1, \dots, x_n)$  and the output sequence is  $Y = (y_1, \dots, y_m)$ . For the encoder RNN, the encoded vector representation is the hidden state  $h_n$  at the last time step of the input sequence. Similarly, for the decoder RNN, the hidden state  $\tilde{h}_t$  at time step  $t$  can be updated based on  $\tilde{h}_{t-1}$  and  $y_t$ , where the hidden state  $\tilde{h}_0$  of the decoder RNN is  $h_n$ .

#### 3.2. RED for Human Motion Prediction

The RED can be applied to human motion prediction which can be regarded as a sequence-to-sequence learning problem. Suppose the given sequence  $X$  has  $n$  frames, i.e.,

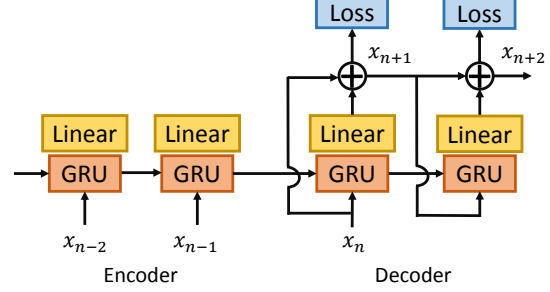


Figure 2. A residual architecture of RNN Encoder-Decoder (RED) [19]. For the encoder, the observed pose is the input at each frame. For the decoder, the input at a particular time step is its own previous prediction (except for the first time step). The decoder has a residual connection which forces the RNN to predict velocities.

$X = (x_1, \dots, x_n)$ , and the predicted future sequence  $Y$  has  $m$  frames,  $Y = (x_{n+1}, \dots, x_{n+m})$ . An RNN structure is used to model the input sequence  $X$  and predict the output sequence  $Y$ . Based on the learned hidden state of the decoder RNN, the future poses can be predicted by using linear regression. Formally, for  $j \in \{1, \dots, m\}$ , the predicted pose at the future  $j$ -th frame is

$$x_{n+j} = Wh_{n+j-1} + b \quad (2)$$

where  $W$  and  $b$  are weight and bias parameters, and when  $j = 1$ ,  $h_n$  is the hidden state of the encoder RNN at the last time step.

While predicting future poses, the mean squared error loss is usually used to train the RED. The minimized loss function of a training sequence is

$$L = \frac{1}{m} \sum_{j=1}^m \|y_{n+j} - x_{n+j}\|_2 \quad (3)$$

where  $y_{n+j}$  is the ground truth pose at time step  $(n+j)$ .

One good structure of RED for human motion prediction is illustrated in Figure 2, where the decoder RNN has a residual connection [19]. The predicted pose at the future  $j$ -th frame is

$$x_{n+j} = x_{n+j-1} + Wh_{n+j-1} + b \quad (4)$$

where  $j \in \{1, \dots, m\}$ , and when  $j = 1$ ,  $x_n$  is the given pose of the input sequence at the last time step.

For human motion prediction, several good practices are exploited with the RED structure [19]. For example, one layer of GRU [6] is computationally inexpensive and achieves very competitive results. The LSTM [12] is inferior to the GRU. Parameter sharing between the encoder RNN and the decoder RNN accelerates convergence. The residual connection ensures continuities between the conditioned sequence and prediction which could improve performance. We feed the prediction instead of the ground truth at each time step to the decoder RNN during training.

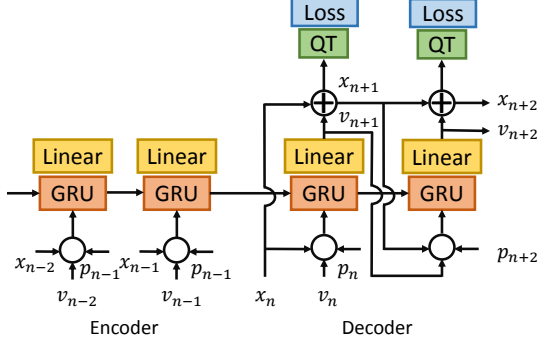


Figure 3. The structure of the Position-Velocity Recurrent Encoder-Decoder (PVRED). Both the encoder and decoder have three types of input: poses  $x_n$ , velocities  $v_n$  and positions  $p_n$ . Here, QT denotes the proposed Quaternion Transformation layer.

## 4. The Proposed Position-Velocity RED

Based on the RED model, we propose a Position-Velocity Recurrent Encoder-Decoder (PVRED) which is shown in Figure 3. Different from RED, our PVRED takes in human poses, pose velocities and position embedding. The encoder takes in the three inputs at each time step, and derives the initial hidden state of the decoder from the given sequence. The decoder first predicts velocities of the next frame, and predicts corresponding poses with a residual connection. The predicted pose velocities and human poses are considered as the input of the decoder at the next time step. We also design a Quaternion Transformation (QT) layer and define a robust loss function of human poses in a unit quaternion space.

### 4.1. Position Embedding

While it is a common practice to incorporate position embedding in many natural language processing tasks, temporal position information is seldom used for computer vision tasks. The positional information encourages the model to learn more discriminative representations as it differentiates the representations of similar poses at different time steps. It also has the potential to alleviate the mean pose problem that the predicted poses converge to an undesired mean pose.

Position embedding is to encode the absolute temporal positions of different frames into a real-valued vector which conveys the relative position information. One simple method is to use one-hot vector where the encoded vector is all zero values except for the index of the current frame, which is marked with one. The one-hot embedding is not flexible for encoding the sequence of a variable length. Inspired by the work [26], we use sine and cosine functions of different frequencies to encode the relative or absolute positions.

Assume that the given sequence has  $n$  frames. We aim to predict the future  $m$  frames. For a time step  $t$ ,

$t \in \{1, \dots, n, \dots, n + m\}$ , the position embedding  $p_t$  is expressed as

$$\begin{aligned} p_t(2i) &= \sin(t/10000^{2i/d^p}), \\ p_t(2i-1) &= \cos(t/10000^{2i/d^p}), \end{aligned} \quad (5)$$

where  $d^p$  is the embedding dimension,  $i$  is the index, and  $1 \leq i \leq \lceil d^p/2 \rceil$ .

Each dimension of the positional embedding is a sinusoid. The wavelengths form a geometric progression from  $2\pi$  to  $10000 \cdot 2\pi$ . For any fixed offset  $k$ ,  $p_{t+k}$  can be represented as a linear function of  $p_t$ . Therefore, the sinusoid embedding method allows the model to learn to attend by relative positions and predict natural-looking poses at different time intervals. It also allows this model to extrapolate to sequences of variable lengths during training.

### 4.2. Position-Velocity RNN

Given the input of human pose  $x_t$  at each time step  $t$ , we consider the time derivative of  $x_t$ , i.e., the velocity of human poses. It is easy to preserve motion continuities in terms of velocity as it directly measures human motion. We combine velocity and position embedding with the input of human poses, and design a Position-Velocity RNN (PVRNN) to predict a sequence of human poses.

The proposed PVRNN has three inputs: human pose  $x_t$ , pose velocity  $v_t$ , and position embedding  $p_t$ . Following the good practice of previous works [19, 11, 20], the unit cell is GRU, which has a reset gate  $r_t$  and an update gate  $z_t$ . The hidden state  $h_t$  at time step  $t$  is computed as

$$\begin{aligned} z_t &= \sigma(U_x^z x_t + U_v^z v_t + U_p^z p_t + W^z h_{t-1}) \\ r_t &= \sigma(U_x^r x_t + U_v^r v_t + U_p^r p_t + W^r h_{t-1}) \\ \tilde{h}_t &= \tanh(U_x^h x_t + U_v^h v_t + U_p^h p_t + W^h (r_t \circ h_{t-1})) \\ h_t &= (1 - z_t) \circ h_{t-1} + z_t \circ \tilde{h}_t \end{aligned} \quad (6)$$

where  $\circ$  denotes the Hadamard product, and variables  $U$  (e.g.,  $U_x^z, U_v^z$ ) and  $W$  (e.g.,  $W^z$ ) are weight matrices.

Given a sequence of history poses  $X = (x_1, \dots, x_n)$ , we aim to predict future poses  $Y = (x_{n+1}, \dots, x_{n+m})$  of the next  $m$  time steps. To estimate the future pose, the velocity is first predicted based on the hidden state and then added to the previous pose. Mathematically,

$$\begin{aligned} v_{n+j-1} &= W h_{n+j-1} + b \\ x_{n+j} &= x_{n+j-1} + v_{n+j-1} \end{aligned} \quad (7)$$

where  $W$  and  $b$  are weights and bias parameters. For the decoder,  $j \in \{1, \dots, m\}$ , and when  $j = 0$ ,  $h_n$  is the last time step of the RNN encoder.

### 4.3. Quaternion Transformation

For human motion prediction, human poses are mostly described by joint rotations using the exponential maps. The exponential map describes the axis and magnitude of

a three DOF rotation, and is numerically stable. Despite the many advantages, the exponential map suffers from singularities (i.e., gimbal lock) and discontinuities in  $R^3$  of radius  $2n\pi$  ( $n = \{1, 2 \dots\}$ ) [10]. The 3D rotations can also be parameterized by unit-length quaternions in  $R^4$ . The quaternions can get rid of singularities and discontinuities, and the multiplication operator in the quaternion space corresponds to matrix multiplication of rotation matrices. The recent work [20] converts the raw input of exponential maps into quaternions and uses RED to predict the future joint rotations with quaternions as well. To enforce the unit length of quaternions, an explicit normalization layer is added to their network. Therefore, their approach requires additional operations of preprocessing and postprocessing and is not end-to-end trainable.

Like most previous works [15, 19, 9, 18, 11], the exponential map of joint rotations is used as the input of the proposed network. To enjoy the benefits of quaternion parameterization, we design a novel Quaternion Transformation (QT) layer to convert the predicted pose from exponential maps to quaternion. The QT layer could be embedded into the end-to-end trainable network. Assume that the human body has  $J$  joints, and  $e_j$  denotes the exponential map of joint  $j$ . The predicted or the ground truth pose at a particular time step is  $x = [e_1^T, \dots, e_i^T, \dots, e_J^T]^T$ . For simplicity, we use  $e$  to denote  $e_j$ , which is a three-dimensional vector. The QT layer transforms  $e$  into a four-dimensional vector  $q$ :

$$q(i) = \begin{cases} \cos(0.5\|e\|_2) & i = 1 \\ \frac{\sin(0.5\|e\|_2)}{\|e\|_2} \cdot e(i-1) & i \geq 2 \end{cases} \quad (8)$$

where  $q$  denotes the corresponding joint rotations in terms of quaternions.

During backpropagation, the derivative of  $q$  with respect to  $e$  is the Jacobian matrix with dimensions  $4 \times 3$ , which is

$$\frac{\partial q}{\partial e} = \begin{bmatrix} \sin(0.5\|e\|_2) \cdot \hat{e}^T \\ 0.5 \cos(0.5\|e\|_2) \cdot E + \frac{\sin(0.5\|e\|_2)}{\|e\|_2} (I_3 - E) \end{bmatrix} \quad (9)$$

where  $I_3$  is the  $3 \times 3$  identity matrix, and

$$\begin{aligned} \hat{e} &= \frac{e}{\|e\|_2} \\ E &= \hat{e} \otimes \hat{e} \end{aligned} \quad (10)$$

where  $\hat{e}$  is the normalized vector of  $e$ ,  $\otimes$  denotes the outer product of two vectors, and  $E$  is a  $3 \times 3$  matrix.

#### 4.4. Training

To train the proposed network, we aim to define a loss function in the unit quaternion space. The objective is to minimize the differences between observed poses and predicted poses and keep the unit length of quaternion representations. The loss function should be robust against outliers while keeping the unit length of quaternions. Here, we

use the mean absolute error loss

$$L = \frac{1}{m} \sum_{j=1}^m \|g(y_{n+j}) - g(x_{n+j})\|_1 \quad (11)$$

where  $g$  denotes the Quaternion Transformation (QT) in Section 4.3,  $x_{n+j}$  is the predicted pose of Equation (7), and  $y_{n+j}$  is the ground truth pose.

During testing, the QT layer and the loss function are discarded. The proposed network takes in human poses, pose velocities and position embedding and predicts future poses. Both human poses and pose velocities are represented by the original exponential map.

## 5. Experiments

We validate our approach on two important benchmarks: Human 3.6M dataset [14] and CMU Motion Capture dataset [1]. Comparisons of our method with the state-of-the-arts are performed and ablation analysis is provided.

### 5.1. Datasets

**Human3.6M.** The Human 3.6M dataset [14] is a large-scale publicly available dataset with 3.6 million accurate 3D poses. Each 3D pose has 32 joints. It is recorded by a Vicon motion capture system, and consists of 15 activities. Both cyclic motions such as walking and non-cyclic motions such as smoking are included. The activities are conducted by seven different subjects, and each subject performs two trials for each activity. The dataset is challenging and widely used in human motion analysis due to large pose variations. We follow the standard experimental setup [7, 15, 19]. The sequences are down sampled by 2 to obtain a frame rate of 25fps. The sequences of the subject indexed 5 are used for testing and the other sequences are used for training. The Euclidean distance between predictions and the ground truth in terms of Euler angle is measured, and the test errors are averaged across 8 different seed clips.

**CMU Motion Capture.** The CMU Motion Capture dataset [1] is a large dataset which provides 3D pose data of 144 different subjects. It contains a large spectrum of movements including everyday movements such as walking and running as well as sport movements such as climbing and dancing. Each pose has 38 joints for this dataset. Similar to [18], we choose actions for human motion prediction based on below criteria. We select single person actions, and remove two person interactions and the composition of several atomic actions. We also exclude the categories which do not provide enough training data. The sequences are down sampled to satisfy the frame rate of 25fps. We use the same train/test split as [18], and calculate the Euclidean distance between predictions and the ground truth in terms of Euler angle. To make the results more stable, we report the averaged distance across 80 sampled seed clips.

Table 1. Short-term prediction error on the Human3.6M dataset. The result is the mean angle error measured at {80, 160, 320, 400} milliseconds after the seed motion.

Milliseconds	Walking				Eating				Smoking				Discussion			
	80	160	320	400	80	160	320	400	80	160	320	400	80	160	320	400
ERD [7]	1.30	1.56	1.84	–	1.66	1.93	2.28	–	2.34	2.74	3.73	–	2.67	2.97	3.23	–
LSTM-3LR [7]	1.18	1.50	1.67	–	1.36	1.79	2.29	–	2.05	2.34	3.10	–	2.25	2.33	2.45	–
SRNN [15]	1.08	1.34	1.60	–	1.35	1.71	2.12	–	1.90	2.30	2.90	–	1.67	2.03	2.20	–
DAE-LSTM [9]	1.00	1.11	1.39	–	1.31	1.49	1.86	–	0.92	1.03	1.15	–	1.11	1.20	1.38	–
Zero-velocity [19]	0.39	0.68	0.99	1.15	0.27	0.48	0.73	0.86	0.26	0.48	0.97	0.95	0.31	0.67	0.94	1.04
Res GRU unsup. [19]	0.27	0.47	0.70	0.78	0.25	0.43	0.71	0.87	0.33	0.61	1.04	1.19	0.31	0.69	1.03	1.12
Res GRU sup. [19]	0.28	0.49	0.72	0.81	0.23	0.39	0.62	0.76	0.33	0.61	1.05	1.15	0.31	0.68	1.01	1.09
RNN-MHU [24]	0.32	0.53	0.69	0.77	–	–	–	–	–	–	–	–	0.31	0.66	0.93	1.00
AGED w/ geo [11]	0.28	0.42	0.66	0.73	0.22	0.35	0.61	0.74	0.30	0.55	0.98	0.99	0.30	0.63	0.97	1.06
TP-RNN [5]	0.25	0.41	0.58	0.65	0.20	0.33	<b>0.53</b>	0.67	0.26	0.47	0.88	0.90	0.30	0.66	0.96	1.04
Conv Seq2Seq [18]	0.33	0.54	0.68	0.73	0.22	0.36	0.58	0.71	0.26	0.49	0.96	0.92	0.32	0.67	0.94	1.01
QuaterNet [20]	0.21	<b>0.34</b>	0.56	0.62	0.20	0.35	0.58	0.70	0.25	0.47	0.93	<b>0.90</b>	0.26	0.60	0.85	0.93
Ours	<b>0.20</b>	0.35	<b>0.54</b>	<b>0.59</b>	<b>0.18</b>	<b>0.32</b>	0.54	<b>0.66</b>	<b>0.22</b>	<b>0.44</b>	<b>0.81</b>	0.91	<b>0.24</b>	<b>0.60</b>	<b>0.83</b>	<b>0.93</b>

Table 2. Long-term prediction error on the Human3.6M dataset. The error is measured at {560, 1000} milliseconds after the seed motion.

Milliseconds	Walking		Eating		Smoking		Discussion	
	560	1000	560	1000	560	1000	560	1000
Zero-velocity [19]	1.35	1.32	1.04	1.38	1.02	1.69	1.41	1.96
ERD [7]	2.00	2.38	2.36	2.41	3.68	3.82	3.47	2.92
LSTM-3LR [7]	1.81	2.20	2.49	2.82	3.24	3.42	2.48	2.93
SRNN [15]	1.90	2.13	2.28	2.58	3.21	3.23	2.39	2.43
DAE-LSTM [9]	1.55	1.39	1.76	2.01	1.38	1.77	1.53	1.73
Res GRU sup. [19]	0.93	1.03	0.95	1.08	1.25	1.50	1.43	1.69
TP-RNN [5]	0.74	0.77	0.84	1.14	0.98	1.66	1.39	1.74
AGED w/ geo [11]	0.89	1.02	0.92	<b>1.01</b>	1.15	1.43	1.33	<b>1.56</b>
Conv Seq2Seq [18]	–	0.92	–	1.24	–	1.62	–	1.86
Ours	<b>0.65</b>	<b>0.66</b>	<b>0.76</b>	1.14	<b>0.97</b>	<b>1.42</b>	<b>1.29</b>	1.77

## 5.2. Implementation Details

Similar to previous works [19, 20, 18], we train a model by using data of all actions, and test the predicted error for each of the selected actions. The action label is not used and the proposed model is action-agnostic. Some works [19, 18] preprocess data by subtracting the mean pose and dividing the standard deviation. We focus on end-to-end training and do not normalize the raw data. Unless otherwise specified, the given past sequence has 50 frames (2 seconds), and the predicted future sequence has 25 frames (1 second). During training, we uniformly sample clips of a fixed length from the training data. The numbers of hidden units of RNN are 1,024 and 512 for the Human3.6M dataset and CMU dataset, respectively. We set the dimension of position embedding the same as the dimension of the original pose.

During training, dropout with a rate of 0.2 is utilized when predicting future poses. We adopt the Adam optimizer with a constant learning rate of 0.0001. Batch training is used with a mini-batch size of 128. The maximum number of training epochs is 20,000. Our implementation is based on PyTorch, and the code will be released soon.

## 5.3. Evaluation on Human3.6M

**Short-Term Prediction.** Following previous convention [15, 11, 18], we consider the prediction less than 500 milliseconds as short-term prediction. Within this time

range, motion is almost deterministic and fairly predictable. In accordance with most previous works [7, 15, 19, 20], we consider four representative actions: walking, smoking, eating, and discussion. Walking is periodic and the other three are aperiodic. Table 1 compares prediction errors with previous approaches on the Human3.6M dataset. Our approach yields the state-of-the-art performance for all actions at different time steps. For example, for walking and at 80 milliseconds, our approach beats the strong baseline Residual RNN [19] by more than 0.07, which is a significant margin when compared with the improvement of the contemporaneous approaches. Our method is also considerably superior to the recent quaternion based RNN [20] which models and predicts human motion in the quaternions space, and the sequence-to-sequence model based on CNN [18].

**Long-Term Prediction.** Motion prediction no less than 500 milliseconds is regarded as long-term prediction, which is more challenging than short-term prediction due to the stochastic nature and uncertainty of human motion. The results on the Human3.6M dataset are given in Table 2. Our approach attains the best results nearly in all the scenarios for both periodic actions and aperiodic actions. Specifically, for walking at 1,000 milliseconds, our approach decreases the reported lowest error, i.e., 0.92 of Conv Seq2Seq [18], by 0.26, and beats the Residual RNN [19] by 0.37. For predictions at 560 milliseconds, our predicted errors are 0.16, 0.18 and 0.04 lower than the best published results for eating, smoking, and discussion, respectively.

**Visualization of Prediction.** We provide qualitative results by visualizing predicted poses of the test data, which are shown in Figure 4. We observe that our approach mitigates the mean pose problem, and makes accurate short-term predictions and natural-looking long-term predictions. We also observe that predictions of RED (i.e., the Residual RNN [19]) freeze to some mean poses and go faraway from the ground-truth in the long term. Let us take walking as an example, predictions of RED converge to a fixed pose at about 600 milliseconds, and the converged pose and the



Table 3. Short-term prediction error on the CMU Motion Capture dataset. The results are averaged over 80 seed motion sequences for each activity on the test set.

Milliseconds	Walking				Washing				Basketball				Jumping			
	80	160	320	400	80	160	320	400	80	160	320	400	80	160	320	400
Res GRU [19]	0.29	0.45	0.66	0.73	0.34	0.66	1.02	1.13	0.42	0.73	1.20	1.35	0.63	0.91	1.44	1.67
Conv Seq2Seq [18]	0.35	0.44	0.45	0.50	0.30	0.47	0.80	1.01	0.37	0.62	1.07	1.18	<b>0.39</b>	<b>0.60</b>	1.36	1.56
Zero-velocity [19]	0.30	0.50	0.80	0.93	0.33	0.53	0.89	1.03	0.48	0.85	1.47	1.71	0.46	0.68	1.22	1.44
Moving avg. 2 [19]	0.32	0.51	0.82	0.94	0.35	0.56	0.91	1.05	0.52	0.90	1.51	1.74	0.49	0.72	1.25	1.46
Ours	<b>0.28</b>	<b>0.34</b>	<b>0.41</b>	<b>0.43</b>	<b>0.25</b>	<b>0.37</b>	<b>0.67</b>	<b>0.81</b>	<b>0.36</b>	<b>0.56</b>	<b>0.95</b>	<b>1.13</b>	0.46	0.65	<b>1.14</b>	<b>1.34</b>

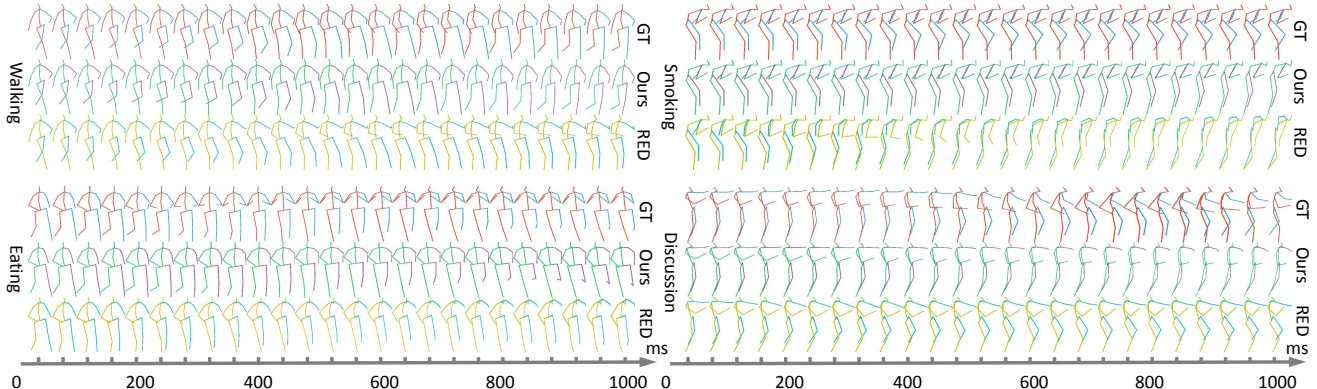


Figure 4. Qualitative predicted poses in the future 1,000 milliseconds after the seed motion. Our predictions are less faraway from the ground-truth than predictions of RED, especially in the long term (e.g., more than 600 milliseconds). Best viewed in color with zoom.

real pose vary considerably. In contrast, our predictions stay close to the ground-truth even in the future 1,000 milliseconds.

We also visualize predicted poses in very long time horizons. As the decoder RNN could generate sequences of variable lengths, we predict future human poses of the next 100 frames (4 seconds) given past poses of 50 frames (2 seconds). The same experimental settings and parameters are used except the length of predicted sequence. After training, we visualize predicted poses of the test samples. Figure 5 shows the results of two representative actions, i.e., periodic walking and aperiodic smoking. We find that our approach could predict human-like and meaningful poses in the future 4,000 milliseconds, while predictions of RED quickly drift away to non-human-like poses. For example, RED predicts strange poses in long time horizons (e.g., more than 1.4 seconds), and our predictions look plausible and show little difference with the real poses.

#### 5.4. Evaluation on CMU Motion Capture

Table 4. Long-term prediction error on the CMU Motion Capture dataset. Our model consistently achieves the best performance.

Milliseconds	Walking		Washing		Basketball		Jumping	
	560	1000	560	1000	560	1000	560	1000
Res GRU [19]	0.80	0.83	1.22	1.23	1.51	1.64	1.87	2.17
Conv Seq2Seq [18]	—	0.78	—	1.39	—	1.95	—	2.01
Zero-velocity [19]	1.10	1.26	1.27	1.53	2.08	2.54	1.75	1.77
Moving avg. 2 [19]	1.11	1.26	1.28	1.53	2.09	2.53	1.76	1.76
Ours	<b>0.47</b>	<b>0.53</b>	<b>1.02</b>	<b>1.20</b>	<b>1.41</b>	<b>1.61</b>	<b>1.57</b>	<b>1.75</b>

The CMU Motion Capture dataset is recently used for

human motion prediction, and there are only a few reported results. We consider an agnostic zero-velocity baseline which constantly predicts the last observed frame [19], and the moving average baseline with a window size of 2 [19]. The two baselines are simple but effective, and outperform many learning based approaches.

**Short-Term Prediction.** Similar to the Human3.6M dataset, we report results for four representative actions: walking, washing (washing window), basketball, and jumping. Jumping is aperiodic, and the other three are periodic. The results are summarized in Table 3. Our approach consistently outperforms the zero-velocity baseline as well as the strong baseline Residual RNN [19]. In most cases, our approach exceeds the recent sequence-to-sequence model based on CNN [19].

**Long-Term Prediction.** The errors of long-term prediction are presented in Table 4. Our results are much better than those of the comparative approaches for both periodic actions and aperiodic actions. For walking and basketball, our approach beats the Zero-velocity [19] baseline by 0.63 and 0.67 at 560 milliseconds, respectively. The experiments further confirm advantages of our approach for long-term predictions.

#### 5.5. Ablation Studies

We run a number of ablations to analyze the proposed model. Without loss of generality, we only give the results on the Human3.6M dataset. The short-term prediction and long-term prediction are summarized in Table 5 and Ta-

Table 5. Ablations of the proposed method for short-term prediction. Here, Var. 1-6 are six ablation methods.

Method	Vel	Pos	QT	Walking				Eating				Smoking				Discussion			
Milliseconds				80	160	320	400	80	160	320	400	80	160	320	400	80	160	320	400
Ours	✓	✓	✓	<b>0.20</b>	<b>0.35</b>	<b>0.54</b>	<b>0.59</b>	<b>0.18</b>	<b>0.32</b>	0.54	<b>0.66</b>	<b>0.22</b>	<b>0.44</b>	<b>0.81</b>	<b>0.91</b>	<b>0.24</b>	<b>0.60</b>	<b>0.83</b>	<b>0.93</b>
Var. 1		✓	✓	0.23	0.38	0.56	0.62	0.21	0.34	<b>0.53</b>	0.68	0.27	0.52	0.90	1.00	0.32	0.70	0.95	1.06
Var. 2	✓		✓	0.21	0.35	0.54	0.59	0.21	0.35	0.55	0.68	0.25	0.50	0.88	0.97	0.27	0.64	0.91	0.98
Var. 3	✓	✓		0.23	0.39	0.59	0.66	0.21	0.36	0.60	0.73	0.28	0.53	0.90	1.03	0.30	0.70	1.03	1.15
Var. 4			✓	0.24	0.40	0.62	0.69	0.23	0.40	0.65	0.79	0.29	0.56	0.98	1.11	0.31	0.68	0.98	1.08
Var. 5		✓		0.25	0.42	0.59	0.68	0.22	0.38	0.62	0.78	0.30	0.56	0.96	1.09	0.33	0.71	0.97	1.07
Var. 6	✓			0.24	0.42	0.62	0.68	0.24	0.41	0.64	0.79	0.34	0.65	1.13	1.29	0.36	0.78	1.16	1.27

ble 6, respectively. For simplicity, pose velocity, position embedding, and quaternion transformation are abbreviated as Vel, Pos and QT, respectively. Different combinations of Vel, Pos and QT correspond to six variants of the proposed method. For example, Var. 1 refers to the approach that utilizes position embedding and quaternion transformation, and Var. 6 is the approach which only applies pose velocity.

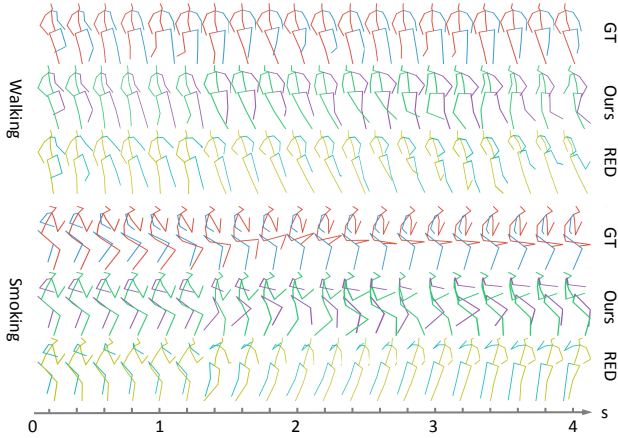


Figure 5. Qualitative predicted poses in the future 4,000 milliseconds after the seed motion.

Table 6. Ablations for the proposed method for long-term prediction on the Human3.6M dataset.

Method	Vel	Pos	QT	Walking		Eating		Smoking		Discussion	
Milliseconds				560	1000	560	1000	560	1000	560	1000
Ours	✓	✓	✓	<b>0.65</b>	<b>0.66</b>	<b>0.76</b>	<b>1.14</b>	<b>0.97</b>	<b>1.42</b>	<b>1.29</b>	1.77
Var. 1		✓	✓	0.70	0.71	0.83	1.19	1.09	1.56	1.44	1.98
Var. 2	✓		✓	0.65	0.68	0.80	1.12	1.03	1.51	1.32	<b>1.72</b>
Var. 3	✓	✓		0.74	0.81	0.87	1.22	1.14	1.64	1.50	1.79
Var. 4			✓	0.75	0.85	0.93	1.30	1.24	1.80	1.47	1.98
Var. 5		✓		0.77	0.84	0.90	1.29	1.21	1.67	1.43	1.81
Var. 6	✓			0.77	0.87	0.95	1.31	1.47	1.98	1.62	1.93

**Pose Velocity.** Comparing our approach with Var. 1, we find that without velocities, the errors increase dramatically for both short-term predictions and long-term predictions. For example, velocity decreases the error by 0.05 for smoking and 0.08 for discussion at 80 milliseconds. It also decreases the error by 0.14 for smoking and 0.21 for discussion at 1000 milliseconds. While comparing Var. 3 and Var. 5, similar conclusions are reached for both periodic actions and aperiodic actions. The results are consistent with our hypothesis in Section 4.2 that velocity preserves motion

continuities and the input of velocity of human motion helps the network predict more accurate potential future poses.

**Position Embedding.** We compare our approach with Var. 2 to examine the effect of position embedding. We find that position embedding improves the results of prediction, and the improvement is even significant for aperiodic actions. For example, position embedding decreases the error by 0.03 at 80 milliseconds for eating, smoking and discussion. It also decreases the error by 0.06 for smoking at 560 milliseconds. We also find Var. 3 shows a substantial decreased error when compared with Var. 6. The results confirm our hypothesis in Section 4.1 that positional information allows the network to learn more discriminative representations, and thus decreases predicted errors.

**Quaternion Transformation.** To analyze the effect of quaternion transformation, we compare our approach with Var. 3 in Table 5 and Table 6 for both short-term prediction and long-term prediction. We find that quaternion transformation significantly contributes to human motion prediction. For example, the QT layer decreases the error by 0.06 for both smoking and discussion at 80 milliseconds. It also decreases the error by 0.22 for smoking at 1000 milliseconds. This significant improvement confirms the benefits of quaternion parameterization which is exempt from singularities and discontinuities (see Section 4.3).

## 6. Conclusion

This paper presents an end-to-end Position-Velocity Recurrent Encoder-Decoder (PVRED) for modeling and predicting human motion dynamics. PVRED incorporates pose velocity, position embedding and quaternion parameterization of human pose into a trainable network and learns to predict future poses based on a sequence of observed frames. Comprehensive experiments show that PVRED outperforms the state-of-the-art approaches for both short-term prediction and long-term prediction. Specifically, PVRED could generate human-like and meaningful poses in the future 4,000 milliseconds after the seed motion of 2,000 milliseconds. Further ablation studies validate the effects of each novel component of PVRED. Future work includes combining PVRED with forward kinematics and inverse kinematics to generate more reliable human poses for long-term prediction.



## References

- [1] CMU Graphics lab motion capture database. <http://mocap.cs.cmu.edu/>.
- [2] K. Ayusawa and E. Yoshida. Motion retargeting for humanoid robots based on simultaneous morphing parameter identification and motion optimization. *IEEE Transactions on Robotics*, 33(6):1343–1357, 2017.
- [3] M. Brand and A. Hertzmann. Style machines. In *Conference on Computer Graphics and Interactive Techniques*, pages 183–192. ACM Press/Addison-Wesley Publishing Co., 2000.
- [4] J. Bütepage, M. J. Black, D. Kragic, and H. Kjellström. Deep representation learning for human motion prediction and classification. In *Conference on Computer Vision and Pattern Recognition*. IEEE, 2017.
- [5] H.-k. Chiu, E. Adeli, B. Wang, D.-A. Huang, and J. C. Niebles. Action-agnostic human pose forecasting. In *Winter Conference on Applications of Computer Vision*. IEEE, 2018.
- [6] K. Cho, B. van Merriënboer, C. Gulcehre, D. Bahdanau, F. Bougares, H. Schwenk, and Y. Bengio. Learning phrase representations using rnn encoder–decoder for statistical machine translation. In *Empirical Methods in Natural Language Processing*, pages 1724–1734, 2014.
- [7] K. Fragkiadaki, S. Levine, P. Felsen, and J. Malik. Recurrent network models for human dynamics. In *IEEE International Conference on Computer Vision*, pages 4346–4354. IEEE, 2015.
- [8] J. Gehring, M. Auli, D. Grangier, D. Yarats, and Y. N. Dauphin. Convolutional sequence to sequence learning. In *International Conference on Machine Learning*, pages 1243–1252. JMLR, 2017.
- [9] P. Ghosh, J. Song, E. Aksan, and O. Hilliges. Learning human motion models for long-term predictions. In *International Conference on 3D Vision*, pages 458–466. IEEE, 2017.
- [10] F. S. Grassia. Practical parameterization of rotations using the exponential map. *Journal of graphics tools*, 3(3):29–48, 1998.
- [11] L.-Y. Gui, Y.-X. Wang, X. Liang, and J. M. Moura. Adversarial geometry-aware human motion prediction. In *European Conference on Computer Vision*, pages 823–842. Springer, 2018.
- [12] S. Hochreiter and J. Schmidhuber. Long short-term memory. *Neural computation*, 9(8):1735–1780, 1997.
- [13] D. Holden, J. Saito, and T. Komura. A deep learning framework for character motion synthesis and editing. *ACM Transactions on Graphics*, 35(4):138, 2016.
- [14] C. Ionescu, D. Papava, V. Olaru, and C. Sminchisescu. Human3.6m: Large scale datasets and predictive methods for 3d human sensing in natural environments. *IEEE Transactions on Pattern Analysis and Machine Intelligence*, 36(7):1325–1339, 2014.
- [15] A. Jain, A. R. Zamir, S. Savarese, and A. Saxena. Structural-rnn: Deep learning on spatio-temporal graphs. In *IEEE Conference on Computer Vision and Pattern Recognition*, pages 5308–5317. IEEE, 2016.
- [16] A. M. Lehrmann, P. V. Gehler, and S. Nowozin. A non-parametric bayesian network prior of human pose. In *IEEE International Conference on Computer Vision*, pages 1281–1288. IEEE, 2013.
- [17] A. M. Lehrmann, P. V. Gehler, and S. Nowozin. Efficient nonlinear markov models for human motion. In *IEEE Conference on Computer Vision and Pattern Recognition*, pages 1314–1321. IEEE, 2014.
- [18] C. Li, Z. Zhang, W. S. Lee, and G. H. Lee. Convolutional sequence to sequence model for human dynamics. In *IEEE Conference on Computer Vision and Pattern Recognition*, pages 5226–5234. IEEE, 2018.
- [19] J. Martinez, M. J. Black, and J. Romero. On human motion prediction using recurrent neural networks. In *IEEE Conference on Computer Vision and Pattern Recognition*, pages 4674–4683. IEEE, 2017.
- [20] D. Pavllo, D. Grangier, and M. Auli. Quaternet: A quaternion-based recurrent model for human motion. In *British Machine Vision Conference*, 2018.
- [21] V. Pavlovic, J. M. Rehg, and J. MacCormick. Learning switching linear models of human motion. In *Advances in neural information processing systems*, pages 981–987, 2001.
- [22] H. Sidenbladh, M. J. Black, and L. Sigal. Implicit probabilistic models of human motion for synthesis and tracking. In *European Conference on Computer Vision*, pages 784–800. Springer, 2002.
- [23] I. Sutskever, O. Vinyals, and Q. V. Le. Sequence to sequence learning with neural networks. In *Advances in neural information processing systems*, pages 3104–3112, 2014.
- [24] Y. Tang, L. Ma, W. Liu, and W. Zheng. Long-term human motion prediction by modeling motion context and enhancing motion dynamic. In *International Joint Conference on Artificial Intelligence*, 2018.
- [25] G. W. Taylor, G. E. Hinton, and S. T. Roweis. Modeling human motion using binary latent variables. In *Advances in Neural Information Processing Systems*, pages 1345–1352, 2007.
- [26] A. Vaswani, N. Shazeer, N. Parmar, J. Uszkoreit, L. Jones, A. N. Gomez, Ł. Kaiser, and I. Polosukhin. Attention is all you need. In *Advances in Neural Information Processing Systems*, pages 5998–6008, 2017.
- [27] R. Villegas, J. Yang, D. Ceylan, and H. Lee. Neural kinematic networks for unsupervised motion retargeting. In *Proceedings of the IEEE Conference on Computer Vision and Pattern Recognition*, pages 8639–8648, 2018.
- [28] H. Wang and L. Wang. Modeling temporal dynamics and spatial configurations of actions using two-stream recurrent neural networks. In *IEEE Conference on Computer Vision and Pattern Recognition*, pages 499–508. IEEE, 2017.
- [29] H. Wang and L. Wang. Beyond joints: Learning representations from primitive geometries for skeleton-based action recognition and detection. *IEEE Transactions on Image Processing*, 27(9):4382–4394, 2018.
- [30] J. Wang, A. Hertzmann, and D. J. Fleet. Gaussian process dynamical models. In *Advances in neural information processing systems*, pages 1441–1448, 2006.